Proceedings of the 9th International Conference on Neural Information Processing (ICONIP'02), Vol. 5
Lipo Wang, Jagath C. Rajapakse, Kunihiko Fukushima, Soo-Young Lee, and Xin Yao (Editors)

CLASSIFYING BRAIN SHAPES

F. Kruggel and V. Kovalev

Max-Planck-Institute of Cognitive Neuroscience
Stephanstrasse 1, D-04103 Leipzig

ABSTRACT

Brain shapes do not necessarily form a continuum in some descriptor space, but may form clusters related to pre-determined genetical factors or acquired diseases. As a feasibility study for introducing a suitable descriptor space, the use of modal analysis was tested on a large brain database acquired in healthy young subjects. Significant shape differences due to gender were found, and intra-gender clusters were determined.

1. INTRODUCTION

The inherent structural complexity and individual variability of the human neocortex left all attempts to construct a computer-based atlas system with a considerable maximal positional uncertainity in the range of 5-15 mm. The three principal approaches use either a single example brain [15], a probabilistic atlas based on a population [10], or try to identify brain structures in the individual scan data directly [8]. All these approaches make the implicit assumption that all brains under study stem from a single cluster in a structural continuum, i.e., a non-linear transformation fulfilling a diffeomorphic contraint is able to transform any instance into another one.

However, it is well-known from neuroanatomy that structural variants of the brain exist, some of which have to be considered as pathologic (e.g., macrogyria or microgyria) or abnormal (e.g., callosal agenesis). But even normal brains exhibit a considerable variability in certain subregions. Since the shape and the size of the head is determined by brain growth - and not vice versa - the brain's shape expression is expected to be governed under some pre-determined genetic control [2]. Indeed, such structural genes for the brain have been identified [12].

Thus, it is questionable, whether brain shapes form a single cluster in this continuum or may better be described by a set of clusters, some of which may be related to gender, ethnic groups, or certain pathologic conditions. If such "brain shape types" exist, they may show differences in the disposition to diseases (e.g., react differently to a traumatic event). In addition, it may be necessary to revise approaches to parcellate the neocortical surface with respect to multiple shape types.

So in the context of this study we were interested whether it is possible and statistically valid to set-up classes of brain shapes in a normal population. To accomplish this, we need to (a) extract the brain from a MRI head scan, (b) describe the brain surface by a set of shape descriptors, and (c) analyze the statistical properties of the brains represented as points in the high-dimensional feature space spanned by the shape descriptors.

There is a rich and well-developed theory for describing shapes [6], and a number of approaches were applied successfully in the medical domain [9, 11, 13]. Just to name a few valid choices for our problem: Fourier descriptors [5], point distribution models [3], spherical harmonics [4], eigen decompositions of non-linear deformations [1]. We selected the so-called "modal matching" which characterizes a study object by the amplitude spectrum of 3D deformation modes required to match it with a reference object.

2. METHODS

With respect to seminal publications of this topic (e.g. [9, 11, 13], we will only cover the basics of modal analysis here. In a nutshell, the brain's shape is represented by a set of salient surface points that are used to set up an biomechanical Finite Element Model (FEM). Modal analysis of this FEM yields a set of 3D deformation modes and amplitudes. Two brains are related to each other by modal matching, i.e., a set of common deformation modes is selected based on point correspondences. By arbitrarily selecting one reference brain, all other brains may be related to the reference in a common coordinate system spanned by a subset of low-frequency deformation modes. This space is used to statistically explore gender differences and cluster brains within gender groups.

2.1. Selection of Node Points

A brain is represented by a set of approximately equally spaced points on its surface $\mathbf{p}$, $\{p_i\}_{i=1,n}, p_i \in \mathcal{R}^3$. The choice of suitable points p_i is critical. We use the follow-

ing algorithm, using a binary voxel volume representing the brain as a single N_{26} connected component as input:

1. Count the number of surface points n_s of the object.
2. If $n_s > n$, scale down the volume by a factor of 2 and proceed with step 1.
3. If $n_s < n$, randomly sample $n - n_s$ surface points from the object at the next higher scale.
4. Mark the corresponding points of the object on all higher scales.

Output is a set of n marked surface points at the original scale.

2.2. Modal Analysis

Consider an object (e.g., a brain) discretized as an isoparametric FEM using the n surface points $\mathbf{p}$ as determined above. The following second order differential equation defines a free, undamped vibration in an isotropical material:

$$\mathbf{M}\ddot{\mathbf{U}} + \mathbf{K}\mathbf{U} = 0 \tag{1}$$

where $\mathbf{U}$ corresponds to a vector of the nodal displacements, $\mathbf{K}$ to the symmetric stiffness matrix, and $\mathbf{M}$ to the mass matrix of the system. Equation 1 is solved as a general positive-definite symmetric eigenvalue problem of size $3n$:

$$\mathbf{K}\mathbf{\Phi} = \mathbf{M}\mathbf{\Phi}\mathbf{\Omega}^2, \tag{2}$$

yielding $\mathbf{\Phi}, \{\phi_i\}_{i=1,3n}$ eigenvectors (called deformation modes) and $\mathbf{\Omega}, \{\omega_i\}_{i=1,3n}$ eigenvalues (the corresponding frequencies). Refer to Sclaroff and Pentland [13] for a detailed description how matrices $\mathbf{M}$ and $\mathbf{K}$ are constructed from the sampled points $\mathbf{p}$.

The vector of nodal shifts $\mathbf{U}$ is related to the amplitudes of the modal deformations $\tilde{\mathbf{U}}$ by:

$$\mathbf{U}(t) = \mathbf{\Phi}\tilde{\mathbf{U}} = \sum_{i=1}^{3n} \tilde{u}_i(t)\phi_i. \tag{3}$$

Modal analysis characterizes a brain represented by n surface points as a set of n deformation modes and their corresponding amplitude spectrum in 3D space.

2.3. Object Comparison

"Modal matching" is a method to computed point correspondences between similar objects. This method is invariant with respect to scaling and translation, and robust to nonrigid deformation and noise. Here, we want to match a set of brains to an arbitrarily chosen reference. More formally, some study object represented by n_s modes $\mathbf{\Phi}_s$ is compared with a reference object described by n_r modes $\mathbf{\Phi}_r$, with generally $n_s \neq n_r$. Following Shapiro und Brady [14] we compute an *affinity matrix* $\mathbf{A} \in \mathbf{R}^{n_r \times n_s}$:

$$a_{i,j} = \| \phi^x_{r,i} - \phi^x_{s,j} \|^2 + \| \phi^y_{r,i} - \phi^y_{s,j} \|^2 + \| \phi^z_{r,i} - \phi^z_{s,j} \|^2,$$

where ϕ^x, ϕ^y and ϕ^z correspond to the three components of a mode ϕ. The smaller the value $a_{i,j}$, the stronger the correspondence between node point i of the study and node point j of the object. We denote a correspondence as strong if $z_{i,j}$ is the minimum of the jth column and $a_{j,i}$ the minimum of the ith row of $\mathbf{A}$.

The modal description of a study relative to a reference is computed from the modal shifts $u_i = p_{r,i} - p_{s,j}$ using the strongly corresponding points $p_{r,i}$ and $p_{s,j}$. For adapting the reference to the study, we search for a minimal squared error applying a minimal deformation energy [13]:

$$E = \left[\mathbf{U}_r - \mathbf{\Phi}_r\tilde{\mathbf{U}}\right]^T \left[\mathbf{U}_r - \mathbf{\Phi}_r\tilde{\mathbf{U}}\right] + \lambda\tilde{\mathbf{U}}^T\mathbf{\Omega}_r^2\tilde{\mathbf{U}}, \tag{4}$$

where λ denotes a Langrange parameter (in our case, $\lambda = 10^{-9}$). Minimization and solving for $\tilde{\mathbf{U}}$ yields:

$$\tilde{\mathbf{U}} = \left[\mathbf{\Phi}_r^T\mathbf{\Phi}_r + \lambda\mathbf{\Omega}_r^2\right]^{-1}\mathbf{\Phi}_r^T\mathbf{U}. \tag{5}$$

Thus, we yield a set of deformation amplitudes $\tilde{\mathbf{U}}, \{\tilde{u_i}\}_{i=1,3n_r}$ that deform the study into the reference, based on the deformation modes $\mathbf{\Phi}_r$ of the reference. Thus, we denote these deformation amplitudes as "shape descriptors", given in a coordinate system spanned by the deformation modes $\mathbf{\Phi}_r$.

Deformation modes may be divided into three groups:

$$\mathbf{\Phi}_r = [\underbrace{\phi_{r,1} \cdots \phi_{r,6}}_{\text{rigid body modes}} \quad \underbrace{\phi_{r,7} \cdots \phi_{r,m}}_{\text{mid-range modes}} \quad \underbrace{\phi_{r,m+1} \cdots \phi_{r,3n_r}}_{\text{higher order modes}}]$$

In order to provide stability against noise, only the mid-range modes are used to construct a modal coordinate system. The shape descriptors sought for are the first m amplitudes $\tilde{u}_i$. We used $m = 60$ for our problem.

3. EXPERIMENTS AND RESULTS

210 subjects (103 male, 107 female, age 24.8 $\pm$ 3.9 years) were selected from our brain data base. A MRI head data set was acquired in each subject on a Bruker 3.0 T Medspec 100 scanner system using a T_1-weighted 3D MDEFT protocol (FOV 220x192x220 mm, matrix 256x128x256, voxel size 0.86x1.5x0.86 mm, scanning time 16 min). Scan data were interpolated to an isotropical voxel size of 1.0 mm by a fourth-order b-spline method, aligned with the stereotactical co-ordinate system while removing the outer hulls of the brain, including the meninges [7]. The brain stem was cut at a level 60 mm below the posterior commissure.

All brains were subjected to a post-processing by unsupervised clustering into foreground (i.e. brain tissue) and

background. The largest connected component in the foreground was extracted, and smoothed by applying by two iterations of a rank filter. The remaining single connected component served as input for the procedure described above. We selected $n = 500$ points to represent the brain surface, and all data sets were referenced to a single, arbitrarily chosen one. We obtained $m = 60$ amplitudes $\tilde{u}_i$ corresponding to deformation modes $\phi_1 \ldots \phi_{60}$ for each data set. Thus, each of the 210 brain shapes is represented by a point in the 60-dimensional coordinate system defined by the rigid-body and mid-range deformation modes.

3.1. Gender-related Differences

The 60 shape descriptors were evaluated for gender-related differences using multiple linear regression (multiple r^2 : 0.4601, F : 2.068 on 60 and 145 degrees of freedom, p : 0.0002), A post-hoc variance analysis yielded the following significantly different modes (see Tab. 1).

Mode	Sum Sq	F value	p-value	
ϕ_{03}	1.3452	7.0267	0.0089	**
ϕ_{05}	0.9449	4.9360	0.0278	*
ϕ_{09}	0.7582	3.9606	0.0484	*
ϕ_{11}	0.9333	4.8753	0.0287	*
ϕ_{13}	- 1.6835	8.7940	0.0035	**
ϕ_{21}	1.6694	8.7205	0.0036	**
ϕ_{23}	- 2.0493	10.7050	0.0013	**
ϕ_{24}	1.5087	7.8807	0.0056	**
ϕ_{43}	0.8948	4.6744	0.0322	*
ϕ_{54}	- 0.9659	5.0457	0.0261	*

Table 1: Significant gender-related differences in the deformation spectrum (* corresponds to $p < 0.05$, ** to $p < 0.01$).

Instead of visualizing a superposition of this deformation mode spectrum, we preferred to find the "most typical" female and male brain by selecting the data set closest to the cluster of female resp. male brains in the mode space. Results are shown in Fig. 1. The most common male is case 79, the most common female case 188.

Then, we classified male and female brain into separate clusters. We computed Euclidean distance matrices using amplitudes $u_7 \cdots u_{60}$ of each individuum. A hierarchical clustering was introduced in the male resp. female group using the Ward agglomeration method. An optimal clustering was achieved with three male and three female classes. Most common cases were: male 0, 51, 62 (see Fig. 2), female 122, 185, 190 (see Fig. 3). The tree plots for both clusterings are shown in Fig. 4 on the last page.

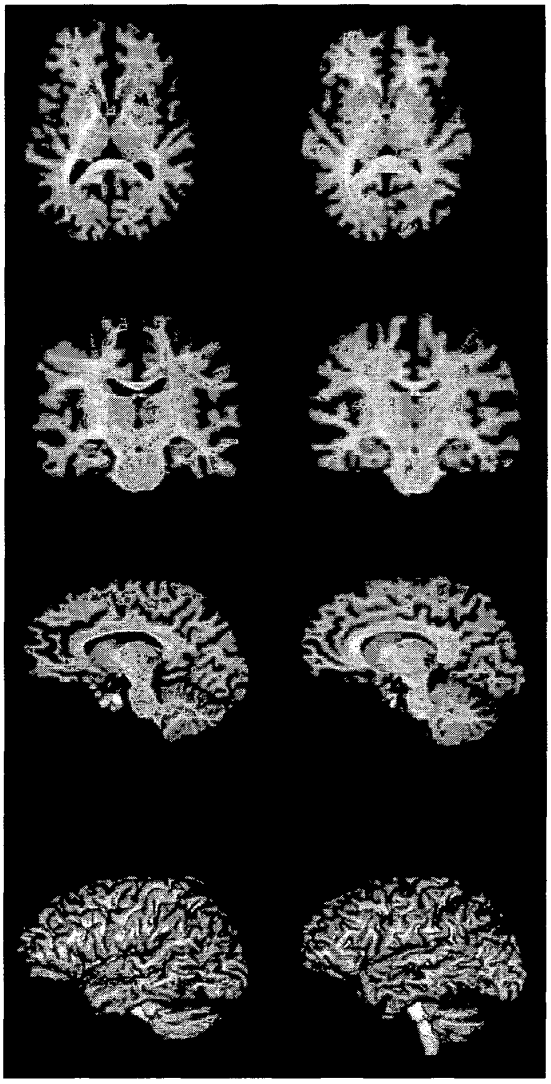

Figure 1: Most typical male (left column) and female data set (right column). Note the difference in the structure of the corpus callosum and the somewhat flatter appearance of the female brain.

4. DISCUSSION

The usefulness of modal analysis as shape descriptors for brains was demonstrated. We found significant gender-related differences and introduced gender-specific classifications. We are aware of the following caveats of our study:

- We used the "outer" brain shape on a rather low resolution level for determination of the modal spectrum.

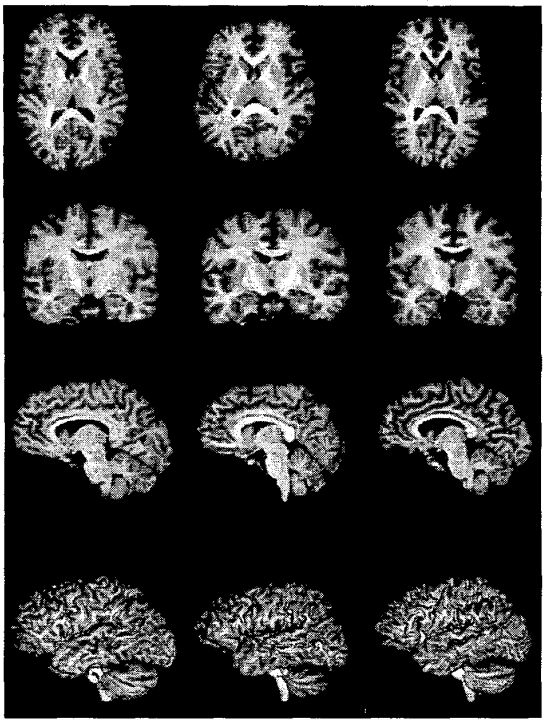

Figure 2: Most typical representatives of the three classes in the male subgroup.

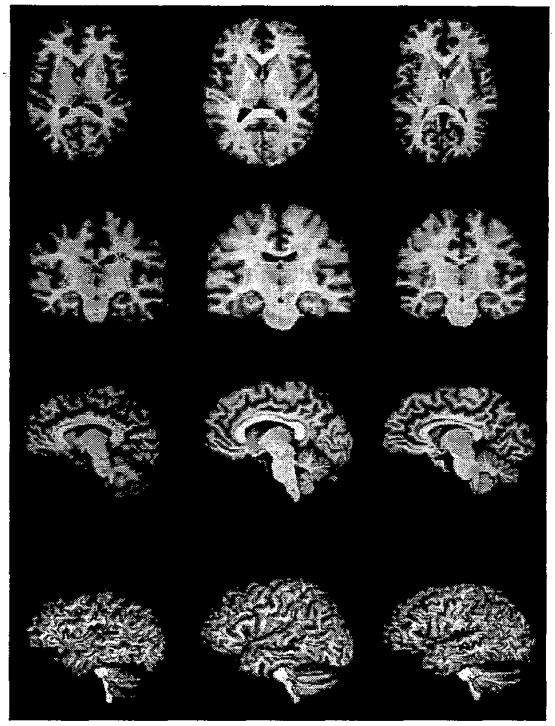

Figure 3: Most typical representatives of the three classes in the female subgroup.

It would be interesting to compare these results with a classification based on a segmentation of the white matter, where the surface description is based on points on the gyral crowns and sulcal fundi. Another classification may be based on the (hypothetical) lissencephalic brain obtained by clipping away all gyri. A comparison of these three classifications may allow distinguishing better between genetic and developmental factors influencing brain shape.

- The classification shown here is valid for the population only. While some results (e.g., the gender-related differences) are expected to generalize (see also [1]), we may expect that even more well-separated clusters are detected if a study includes different ethnic groups [16].
- Point correspondences are based on Euclidean distance in this study. A better approach would use anatomically defined correspondences (i.e., homologue loci).
- A more thorough understanding of the obtained classification in terms of brain organization needs to be performed. Do these shape differences play a role in the relative size of brain compartments (i.e., lobes, gyral volume)?

Another interesting option is to study the progress of neurodegenerative diseases (e.g., Alzheimer's disease) in time-series images which should reveal specific anatomical regions where the atrophying process takes place.

Modal analysis as performed here appears as an easy and attractive means of obtaining shape descriptors, which may serve for a quantitative statistical analysis of biological objects in longitudinal or cross-section studies.

5. REFERENCES

[1] J. Ashburner, C. Hutton, R. Frackowiak, I. Johnsrude, C. Price and K. Friston, Identifying global anatomical differences: deformation-based morphometry. *Human Brain Mapping* 6, 348-57 (1998).

[2] A.J. Bartley, D.W. Jones and D.R. Weinberger, Genetic variability of human brain size and cortical gyral patterns *Brain* 120, 257-269 (1997).

[3] T.F. Cootes, C.J. Taylor, D.H. Cooper and J. Graham, Active shape models - their training and application. *Computer Vision and Image Understanding* 61, 38-59 (1998).

[4] S. Dauber, J. Raczkowsky, J. Brief, S. Hassfeld and H. Worn, Statistical analysis of the morphology of three-dimensional objects and pathologic structures using spherical harmonics. *Studies in Health, Technology and Informatics* 81, 103-105 (2001).

[5] K. Delibasis, P.E. Undrill and G.G. Cameron, Designing Fourier descriptor-based geometric models for object interpretation in medical images using genetic algorithms. *Computer Vision and Image Understanding* 66, 286-300 (1997).

[6] I.L. Dryden and K.V. Mardia, *Statistical Shape Analysis*, Wiley, Chichester, 1998.

[7] F. Kruggel and D.Y. von Cramon, Alignment of magnetic-resonance brain datasets with the stereotactical coordinate system. *Medical Image Analysis* 3, 1-11 (1999).

[8] J.F. Mangin, V. Frouin, I. Bloch, J. Rgis and J. Lpez-Krahe, From 3D magnetic resonance images to structural representations of the cortex topography using topology preserving deformations. *Journal of Mathematical Imaging and Vision* 5, 297-318 (1995).

[9] J. Martin, A. Pentland, S. Sclaroff and R. Kikinis, Characterization of neuropathological shape deformations, *IEEE Transactions on Pattern Analysis and Machine Intelligence* 20, 97-112 (1998).

[10] J.C. Mazziotta, A.W. Toga, A. Evans, P.T. Fox and J.L. Lancaster, A probabilistic atlas of the human brain: theory and rationale for its development. *NeuroImage* 2, 89-101 (1995).

[11] C. Nastar and N. Ayache, Classification of nonrigid motion in 3D images using physics-based vibration analysis, *IEEE Workshop on Biomedical Image Analysis (Seattle)*, pp. 61-69, IEEE Press, Los Alamitos, 1994.

[12] S.M. Pulst, *Neurogenetics.* Oxford University Press, Oxford, 1999.

[13] S. Sclaroff and A. Pentland, Modal matching for correspondence and recognition, *MIT Media Laboratory Perceptual Computing Section*, Technical Report No. 201, (1993).

[14] L.S. Shapiro and M. Brady, Feature-based correspondence: an eigenvector approach, *Image and Vision Computing* 10, 283-288 (1992).

[15] J. Talairach and P. Tournoux, *Co-Planar Stereotactic Atlas of the Human Brain.* Thieme, Stuttgart, 1988.

[16] K. Zilles, R. Kawashima , A. Dabringhaus, H. Fukuda and Th. Schormann, Hemispheric shape of European and Japanese brains: 3D MRI analysis of intersubject variability, ethnical and gender differences, *NeuroImage* 13, 262-271 (2001).

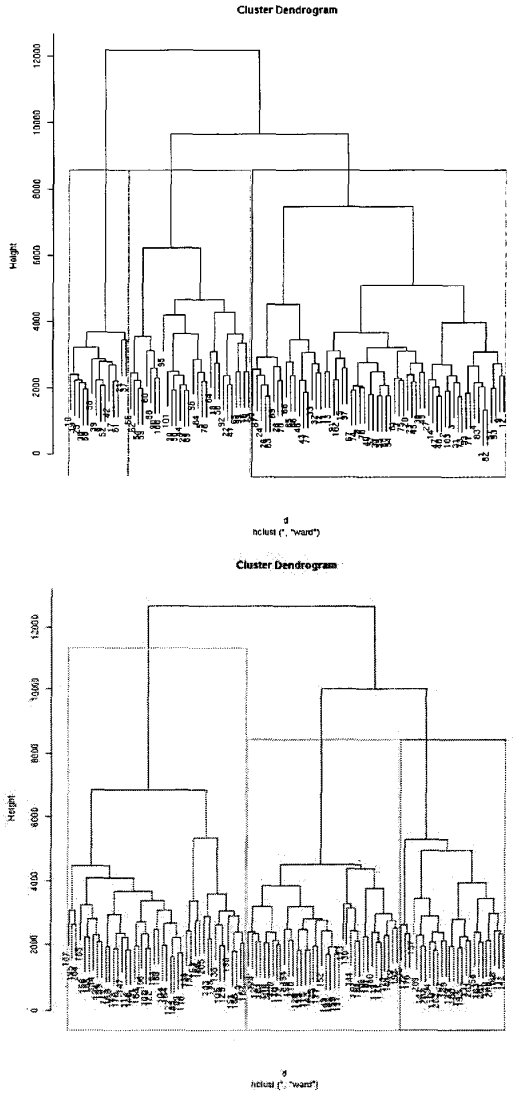

Figure 4: Classification tree for male (top) and female (below) subjects.